CROMER, D. T. & LIBERMAN, D. (1970). *J. Chem. Phys.* **53**, 1891–1898.
CROMER, D. T. & MANN, J. B. (1968). *Acta Cryst.* A**24**, 321–324.
DAHL, L. F., ISHISHI, E. & RUNDLE, R. E. (1957). *J. Chem. Phys.* **26**, 1750–1751.
HARALDSEN, H. (1935). *Z. Anorg. Allg. Chem.* **221**, 397–417.
JEITSCHKO, W. (1974). *Acta Cryst.* B**30**, 2565–2572.
JEITSCHKO, W. & DONOHUE. P. C. (1972). *Acta Cryst.* B**28**, 1893–1898.
JEITSCHKO, W. & DONOHUE. P. C. (1975). *Acta Cryst.* B**31**, 574–580.
JEITSCHKO, W. & RÜHL, R. (1979). *Acta Cryst.* B**35**, 1953–1958.
RÜHL, R. & JEITSCHKO, W. (1980). *Z. Anorg. Allg. Chem.* **466**, 171–178.
RÜHL, R. & JEITSCHKO, W. (1981). *Acta Cryst.* B**37**, 39–44.
RÜHL, R. & JEITSCHKO, W. (1982). *Inorg. Chem.* **21**, 1886–1891.
RÜHL, R., JEITSCHKO, W. & SCHWOCHAU, K. (1982). *J. Solid State Chem.* In the press.
RUNDQVIST, S. (1966). *Acta Chem. Scand.* **20**, 2075–2080.
SHELDRICK, G. M. (1976). *SHELX* 76. A program for crystal structure determination. Univ. of Cambridge, England.

Acta Cryst. (1982). B**38**, 2788–2792

A New Form of Sodium Kurrol Salt studied by the Rietveld Method from X-ray Diffraction Data

BY ATTILIO IMMIRZI AND WILLIAM PORZIO

Facoltà di Ingegneria della Università, 84100 *Salerno, Italy and Istituto di Chimica delle Macromolecole del CNR, via A. Corti* 12, 20133 *Milano, Italy*

(*Received* 7 *September* 1981; *accepted* 8 *June* 1982)

Abstract

A new form of sodium Kurrol salt, sodium metaphosphate, $(NaPO_3)_n$, obtained by finely grinding samples of the *B* form, has been studied by the Rietveld method from powder X-ray diffraction data. Only by using constrained refinement does convergence occur. A comparison between two distinct models is made and the importance of reducing the number of variables is demonstrated. [Crystal data for the two models refined in $I4_1/a$ are: (model I) $a = b = 13{\cdot}177\ (5)$, $c = 5{\cdot}940\ (3)$ Å; (model II) $a = b = 13{\cdot}176\ (6)$, $c = 5{\cdot}931\ (3)$ Å.]

Introduction

In recent papers (Immirzi, 1978, 1980*a*) one of the authors discussed the advantages of combining the Rietveld procedure of refining a structure by means of powder diffraction patterns (Rietveld, 1967, 1969) with the use of constrained variables, for either neutron or X-ray diffraction. In addition a new general-purpose computer program using the generalized-coordinate approach was illustrated and it was shown how polymeric structures can profitably be handled (Immirzi, 1980*a*, *b*; Young, Lundberg & Immirzi, 1980).

Polymeric phosphates already studied by single-crystal techniques have been considered for testing purposes. The different parameter sets obtained with various constrained models and powder patterns can be compared with the single-crystal parameter set, thus providing a check on both parameter reliability and refinement convergence. In particular, the polymeric phosphate $Na_3H(PO_3)_4$, studied by Jost (1968) by single-crystal techniques, was studied again by the Rietveld method using X-ray diffraction data (Immirzi, 1980*b*). The importance of using constrained-variable models was duly demonstrated.

The study of polymeric $NaPO_3$, Kurrol salt, of which two forms are known, *A* type (Jost, 1961) and *B* type (Jost, 1963), was undertaken as a further contribution in this direction. Unexpectedly, however, prolonged grinding of *B*-form samples gave rise to a new polymorph which we termed *C* type whose structure was elucidated using powder diffraction data and refined by the Rietveld method with X-ray radiation.

Although the lack of a single-crystal parameter set does not allow a comparison as for the $Na_3H(PO_3)_4$ structure to be carried out, the critical role of constrained parameters was again demonstrated, using to this end two different constrained models.

Experimental

A sample of Kurrol salt *B* type, kindly supplied by Dr K. H. Jost, was finely ground using a micro ball mill.

0567-7408/82/112788-05$01.00

Table 1. *Experimental details of X-ray diffraction powder-profile measurement of* Na-*Kurrol salt type C*

Instrument	Philips PW-1050 goniometer equipped with step-scan attachment, proportional counter and Soller slits
Radiation	Cu $K\alpha$, Ni-filtered
Divergence slit	0·5° from $2\theta = 5$ to $2\theta = 19{\cdot}5°$; 1° above; rescaling through an overlap margin 19·5–23°
Receiving slit	0·1°
Step width	0·05° (2θ)
Count time	100 s per step
2θ range	from 5 to 60°

Since most particles assumed a needle-shaped form, preferred-orientation effects were feared. To try to avoid them, we had recourse to the same technique already applied in the cited case of $Na_3H(PO_3)_4$, *viz* blending the powder with Technovit 4030-B (a liquid acrylic resin which polymerizes giving a solid non-crystalline product) and cutting the resulting solid material into small particles (~0·1 mm size). X-ray diffraction measurements were then performed according to the specifications given in Table 1.

A comparison between the diffraction scan so obtained (see Fig. 1)* and that of the pure material (see Fig. 2) reveals marked differences. The peaks corresponding to strong *hk*0 reflections at $2\theta = 27{\cdot}0°$ (400), $2\theta = 30{\cdot}4°$ (240 + 420) and $2\theta = 19{\cdot}1°$ (220) are all enhanced in the absence of resin. Actually, needle-like crystals will tend to arrange themselves in the sample holder parallel to the holder basis, so rendering more frequent the occurrence of the Bragg condition for *hk*0 reflections, whose diffraction planes all contain the 00*l* needle axis.

* The numbered intensity of each measured point on the profile, as a function of scattering angle, has been deposited with the British Library Lending Division as Supplementary Publication No. SUP 36978 (6 pp.). Copies may be obtained through The Executive Secretary, International Union of Crystallography, 5 Abbey Square, Chester CH1 2HU, England.

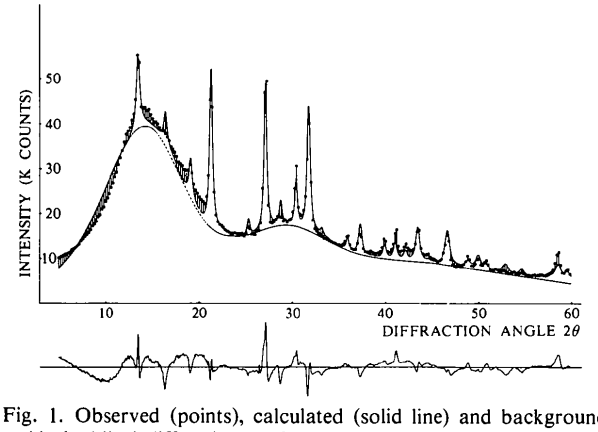

Fig. 1. Observed (points), calculated (solid line) and background (dashed line) diffraction profiles for Na-Kurrol salt *C* type at the end of Rietveld refinement according to model II (fixed bond lengths and local C_{2v} symmetry on P atoms). Only one observed point every four is represented for clarity.

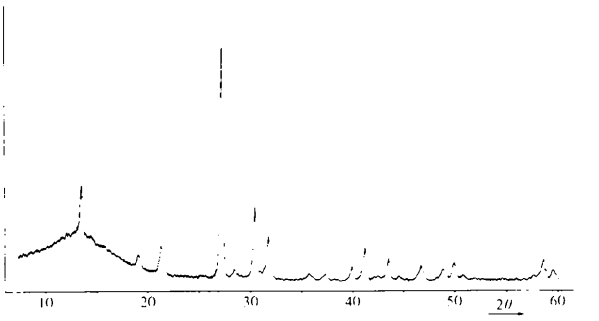

Fig. 2. Diffraction powder spectrum (graphical recording) for Na-Kurrol-*C* *before* blending with Technovit resin. Note the enhanced intensity at $2\theta = 27{\cdot}1°$ with respect to $2\theta = 31{\cdot}8°$,

Structure determination

The experimental diffraction profile matched neither the one calculated for the published single-crystal structure of Na-Kurrol-*B* (Jost, 1963) nor that for Na-Kurrol-*A* (Jost, 1961), and the existence of a new form was accordingly inferred. As, however, the phase transformation takes place in the solid state, the new chain structure was not likely to differ much from that of the *B* form in which the isolated $(PO_3)_n$ chains, as well as the Na^+ cations, obey roughly a 4_1 helix symmetry. On this assumption we tried indexing the powder scan on the basis of a tetragonal unit cell having the *c* edge equal to the *b* edge of the type-*B* cell and the same volume (eight $NaPO_3$ units per cell), but the attempt was not successful. If instead *a* and *b* edges are considered to be $\sqrt{2}$ times as long (*i.e.* twice as large a volume and sixteen $NaPO_3$ units per cell), all resolved peaks were indexable according to a body-centered lattice ($h + k + l = 2n$). This prompted the attractively simple hypothesis of a structure with $I4_1/a$ crystal symmetry. The $I4_1/a$ structure can be reached as a result of adjacent layers of helices sliding with respect to one another along the [101] direction and a very moderate adjustment of atoms within the chain. The subsequent analysis (see *Results and discussion* below) showed that, during the phase transformation, helices maintain their relative orientation within the layers.

A first-approximation 4_1 chain model was obtained from the *B*-type structure. Then trial-and-error calculations were carried out, systematically varying both chain orientation and chain *z* position. Such a structure, which gave a rough agreement with the experimental scan, was then used for subsequent structure refining carried out by the Rietveld method.

Constrained refinement

According to the $I4_1/a$ model the asymmetric structural unit consists of a single $NaPO_3$ unit. With the

modest resolution of the X-ray powder spectrum used, the Rietveld refinement does not converge if the 15 atomic coordinates are refined as independent quantities. Instead, when constraints are introduced, the variables reduce to 11 or 8 and convergence is satisfactory.

Constrained refinement was undertaken with a general-purpose program already described, which uses generalized coordinates (Immirzi, 1978, 1980*a*). While the sodium cation coordinates were adjusted as independent quantities, the anionic chain of 4_1 symmetry was treated using the approach devised for the 3_1 helix of isotactic polypropylene (Immirzi, 1980*a*). The helix structure is defined (see Fig. 3) by the bond lengths l_1, l_2, l_3, the angle φ, the ratio $\tau = r_2/r_1$ and the four bond angles θ_1, θ_2, θ_3, θ_4; the helix orientation by the Φ angle (overall rotation) and z_P (z coordinate of the P atom). By imposing l_1, l_2, l_3 to have fixed canonical values, one obtains an 11-variable model having fixed bond lengths and free bond angles (model I). By imposing the further condition $\theta_1 = \theta_2 = \theta_3 = \theta_4$ (*i.e.* assuming local C_{2v} symmetry on the phosphorus atom) and eight-variable model (model II) results.

Rietveld refinement was carried out successfully with both models. The quantity minimized was $\chi^2 = \sum w_i(I_{obs} - I_{calc})^2$ with w_i set equal to (number of counts)$^{-1}$. I_{calc} was considered to be inclusive of the background intensity and of the contribution of the amorphous resin added. The functional form of I_{calc} was that of Rietveld except for the use of the more flexible Pearson-VII profile function (see Immirzi, 1980*a*, p. 2379).

Besides the above generalized coordinates, the adjusted parameter set includes: (i) the two lattice constants (squared reciprocal); (ii) the U, V, W profile-width parameters of the formula $H_k^2 = U \times \tan^2\theta + V \tan\theta + W$ (Caglioti, Paoletti & Ricci, 1958); (iii) the overall scale factor; (iv) five background intensities at fixed 2θ values; (v) a scale factor for adding the contribution of the amorphous resin blended; the last contribution was evaluated as the sum of two Gaussian profiles of equal width (8·46°) centered at $2\theta = 15{\cdot}96°$ and $2\theta = 30{\cdot}46°$ and having intensity ratio 1/0·817 as determined in separate experiments (see Immirzi, 1980*a*, Fig. 2); (vi) the zero correction for 2θ values; (vii) the peak asymmetry parameter P (see Table 2, note *a*). The isotropic thermal parameters were kept fixed and equal to the values published for the type-*B* single-crystal study.

In both constrained models, parameter adjustment was carried out by varying first the non-structural parameters with structure fixed, then the structural parameters with the non-structural ones fixed, then all parameters together.

Only the Pearson m exponent was adjusted by making a separate refinement of scale factor, U, V, W parameters, background parameters and m itself. The convergence value $m = 1{\cdot}02$ (corresponding to a Cauchy distribution function) was kept fixed in subsequent refinements of all variables.

As some parameters, especially τ and φ, undergo a marked shift oscillation, the final cycles of least-squares refinement were performed by cutting all shifts greater than $0{\cdot}3\sigma$ (σ = standard error) by 75%. In final cycles the shift-to-σ ratio was $<0{\cdot}5$ for both models.

Starting from the best result obtained with model II, we again attempted the Rietveld refinement using the 15 atomic coordinates as unconstrained variables (keeping all the non-structural parameters constant). Even this trial was unsuccessful owing to variable divergence.

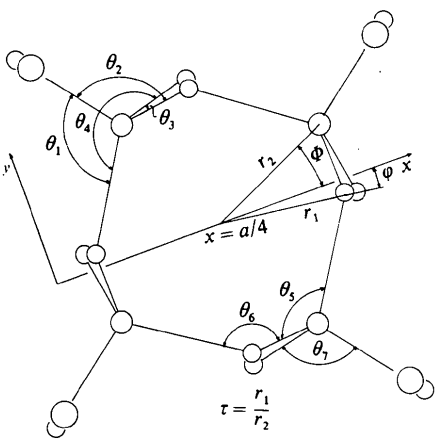

Fig. 3. The generalized coordinates used for describing the anionic part of Na-Kurrol-*C* crystal structure. The chain conformation is arbitrary. For Na^+ cations the ordinary Cartesian coordinates were used.

Results and discussion

Table 2 shows the convergence parameters at the end of the Rietveld refinement carried out according to the two said models. Other structural data are also given; atomic coordinates and standard errors in both cases are listed in Table 3.

From the lattice constants, which are almost insensitive to the choice of the model, the crystal density is calculated to be 2·636 g cm^{-3}, a little higher than in the *B* form (2·610 g cm^{-3}), suggesting that the new form is the more stable.

The two resulting coordinate sets differ appreciably in atomic positions (see Table 3). Although the first model yields the lower value for the R_p and R_{wp} agreement indices, the more constrained model seems to be the only reliable one considering the more realistic θ bond angles resulting (see Table 2), which are all close to values observed in type-*A* and type-*B* cases.

The reduced χ^2 at the end of refinement (see Table 2) considerably exceeds the value 1·0 expected for a

Table 2. *Convergence parameters at the end of constrained Rietveld refinement*

Model I: fixed bond lengths and free bond angles; model II: fixed bond lengths and local C_{2v} symmetry on P atoms. E.s.d.'s (in parentheses) are those obtained from the diagonal terms of the inverse normal-equation matrix. Fixed quantities are $l_1 = l_2 = 1{\cdot}600$ Å, $l_3 = 1{\cdot}476$ Å; $\lambda = 1{\cdot}5418$ Å; $B_{iso} = 1{\cdot}76$ (Na^+), 0·79 (P), 1·13 (chain O), 1·68 (side O) Å^2.

		Model I	Model II
Non-structural parameters			
Scale factor[I]		1·726 (35)	1·904 (46)
Squared reciprocal constants (Å^{-2} × 100)	$a^{-2} = b^{-2}$	0·14398 (11)	0·14402 (13)
	c^{-2}	0·70844 (69)	0·71069 (69)
Zero correction for 2θ (°)		−0·025 (11)	−0·022 (12)
Peak asymmetry parameter P[II]		−0·160 (14)	−0·088 (18)
Profile-function and profile-width parameters[III]	U	5·21 (81)	5·32 (94)
	V	−2·90 (45)	−2·70 (52)
	W	0·494 (62)	0·455 (71)
	m	1·02 (8)	1·02 (8)
Background intensities (k counts) at	$2\theta = 5{\cdot}0°$	2·43 (18)	2·38 (20)
	$= 23{\cdot}5°$	11·46 (16)	11·40 (17)
	$= 34{\cdot}0°$	10·66 (14)	10·69 (15)
	$= 45{\cdot}5°$	9·40 (10)	9·08 (10)
	$= 60{\cdot}0°$	4·96 (10)	4·36 (11)
Scale factor for adding the contribution of the amorphous resin added		10·74 (10)	10·76 (10)
Structural parameters (see Fig. 3)			
τ		1·366 (65)	1·083 (37)
φ (°)		65·3 (7)	59·7 (7)
Φ (°)		−43·0 (8)	−52·6 (5)
z_p (Å)		−0·49 (3)	−0·37 (2)
θ_1 (°)		169·4 (20)	110·0 (8)
θ_2 (°)		96·8 (32)	110·0 (8)
θ_3 (°)		98·8 (24)	110·0 (8)
θ_4 (°)		144·6 (28)	110·0 (8)
x_{Na} (Å)		5·09 (3)	5·30 (2)
y_{Na} (Å)		−2·45 (2)	−2·13 (2)
z_{Na} (Å)		2·60 (3)	2·08 (2)
Disagreement indices (%)			
$R_p = \Sigma \lvert I_{obs} - (1/c) I_{calc} \rvert / \Sigma I_{obs}$		5·5	6·3
$R_{wp} = \{\Sigma w [I_{obs} - (1/c) I_{calc}]^2 / \Sigma w I_{obs}^2\}^{1/2}$		7·1	7·9
Disagreement indices based on net I_{obs} ($I_{obs} = I_{obs}$ − background) (%)			
$R'_p = \Sigma \lvert I_{obs} - (1/c) I_{calc} \rvert / \Sigma I_{obs}$		46·0	47·1
$R'_{wp} = \{\Sigma w [I_{obs} - (1/c) I_{calc}]^2 / \Sigma w I_{obs}^2\}^{1/2}$		36·3	38·0
$[\chi^2/(N-P)]^{1/2}\{\chi^2 = \Sigma w [I_{obs} - (1/c) I_{calc}]^2\}$		9·8	10·3
Other non-structural quantities related to the preceding ones			
Lattice constants	$a = b$ (Å)	13·177 (5)	13·176 (6)
	c (Å)	5·940 (3)	5·931 (3)
Bond angles (see Fig. 3)	θ_5 (°)	90·6 (28)	114·4 (12)
	θ_6 (°)	120·7 (35)	120·5 (12)
	θ_7 (°)	80·3 (30)	106·5 (10)

Notes: (I) From absolute intensities to k count intensities. (II) According to the Rietveld formula, $1 + P|2\theta_l - 2\theta_k|(2\theta_l - 2\theta_k)/\tan\theta_k$. (III) U, V, W control the half-height peak-width according to the formula (Caglioti *et al.*, 1958) $H_k^2 = U\tan^2\theta + V\tan\theta + W$; m is the exponent in the Pearson-VII formula; it was adjusted in a separate refinement together with the variables U, V, W, scale factor and background parameters.

normal distribution of $I_{obs} - I_{calc}$ differences.* If such values are normally distributed ($x = I_{obs} - I_{calc}$):

$$\varphi(x) = \frac{1}{\sigma\sqrt{2\pi}} \exp\left[-\frac{(x-\bar{x})^2}{2\sigma^2}\right]$$

and the integrated distribution function is

$$\Phi(x) = \int_{-\infty}^{x} \varphi(x)\,dx = \tfrac{1}{2} + \tfrac{1}{2}\,\mathrm{erf}\,\frac{x-\bar{x}}{\sqrt{2}\sigma}.$$

Hence the plot of $\mathrm{erf}^{-1}[2\Phi(x) - 1]$ *vs* x must be a straight line with slope $1/\sqrt{2}\sigma$ if the distribution is truly Gaussian. Fig. 4 shows this plot for the present case obtained by grouping the $N = 1100$ differences in 81 groups with $\Delta x = 100$ counts. The almost linear graph confirms that the distribution is truly normal with $\sigma = 1060$ counts.

The discrepancy $\chi^2 > (N - P)$ is therefore indicative that the differences $I_{obs} - I_{calc}$ are not only due to errors in measurements of I_{obs} but also to inaccuracy of I_{calc} terms. Indeed, the assumption both that profiles obey a Pearson function and that peak widths depend only on the 2θ diffraction angle through Caglioti's formula are, for X-ray radiation, of limited validity. Nevertheless, since structural parameters affect only

* This discussion was added after some critical observations from one of the referees.

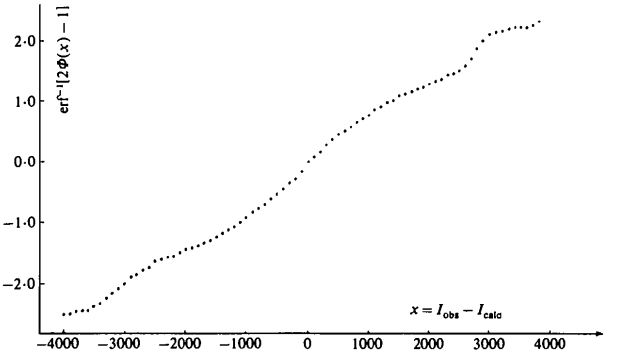

Fig. 4. Distribution of $x = I_{obs} - I_{calc}$ differences. The 1100 variates were grouped in 81 intervals with $\Delta x = 100$ counts. For each interval the value $\mathrm{erf}^{-1}[2\Phi(x) - 1]$ is reported, $\Phi(x)$ being the integral distribution function.

Table 3. *Atomic coordinates with e.s.d.'s in parentheses for models* I *and* II

Atom-to-atom displacements (Å) between the two models are also given.

	Model I			Model II			I − II
	x	y	z	x	y	z	displacement
Na	0·3865 (22)	−0·1856 (13)	0·4379 (43)	0·4021 (15)	−0·1619 (15)	0·3509 (41)	0·63
P	0·3423 (18)	−0·0861 (18)	−0·0827 (52)	0·3266 (16)	−0·1002 (19)	−0·0623 (26)	0·30
O	0·3356 (34)	0·0350 (19)	−0·0952 (62)	0·3655 (27)	0·0145 (17)	−0·0830 (39)	0·48
O′	0·3681 (90)	−0·1951 (23)	−0·0843 (263)	0·4137 (41)	−0·1705 (28)	−0·0691 (138)	0·69
O″	0·3312 (71)	−0·1074 (55)	−0·3254 (56)	0·2618 (41)	−0·1258 (48)	−0·2572 (44)	1·03

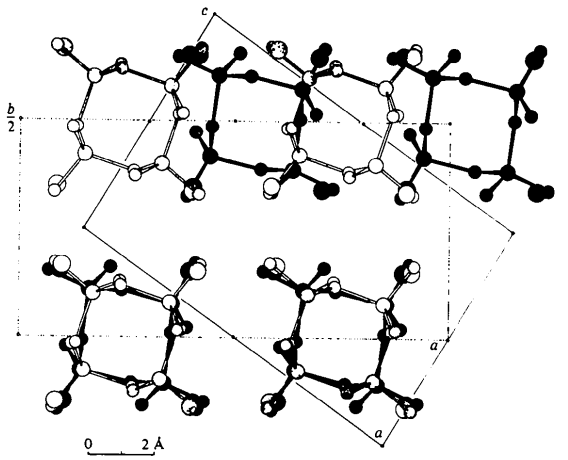

Fig. 5. Na-Kurrol-*C* structure (lighter circles and sticks) overlapped with *B*-type structure (darker circles and sticks) showing the structural relationship between the two forms.

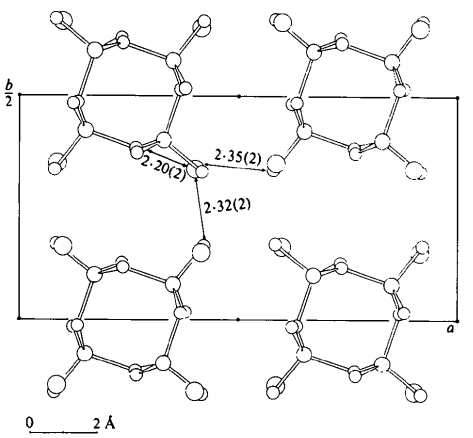

Fig. 6. Crystal packing for Na-Kurrol-*C* salt. The shortest Na···O distances are indicated.

the structure factors through an exact analytical relationship, we can have confidence in the refined structural parameters even if we are very critical in attributing physical significance to *U*, *V*, *W* and *m* parameters.

As shown in Fig. 5, the present structure is closely related to the *B*-type structure. The present helix-to-helix shortest distance [$\frac{1}{2}a$ = 6·58 (2) Å] is almost equal to that observed in the *B* type (6·59 Å). Furthermore, the mutual orientation of the nearest helices [*i.e.* those separated by the ($\frac{1}{2}y0$) inversion centers in the *B* type] remains unchanged, the only structural difference consisting in the relative position of layers of helices parallel to the [101] direction. In the *B*-type structure normal to this direction the helix-to-helix distance is actually larger; so the helix creep takes place just normal to the direction of the weaker intermolecular interactions.

The examination of crystal packing (see Fig. 6) in the present case shows that each sodium cation interacts with three different chains with the shortest Na···O distances 2·16 (2), 2·19 (2), 2·32 (2) Å. In the *B* type the two structurally independent Na^+ cations show a similar behavior, but with larger separations, namely 2·27, 2·35, 2·48 Å. Also the tighter packing seems indicative of a higher stability of the *C* form compared with the *B* form.

The authors are grateful to Dr K. H. Jost for having kindly supplied a sample of sodium Kurrol salt and for useful information.

References

CAGLIOTI, G., PAOLETTI, A. & RICCI, F. P. (1958). *Nucl. Instrum.* **3**, 223–228.
JOST, K. H. (1961). *Acta Cryst.* **14**, 844–847.
JOST, K. H. (1963). *Acta Cryst.* **16**, 640–642.
JOST, K. H. (1968). *Acta Cryst.* B**24**, 992–995.
IMMIRZI, A. (1978). *Acta Cryst.* A**34**, S348–S349.
IMMIRZI, A. (1980*a*). *Acta Cryst.* B**36**, 2378–2385.
IMMIRZI, A. (1980*b*). *Gazz. Chim. Ital.* **110**, 381–387.
RIETVELD, H. M. (1967). *Acta Cryst.* **22**, 151–152.
RIETVELD, H. M. (1969). *J. Appl. Cryst.* **2**, 65–71.
YOUNG, R. A., LUNDBERG, J. L. & IMMIRZI, A. (1980). In *Fiber Diffraction Methods, ACS Symp. Ser.* No. 141, ch. 5, pp. 69–91.